Theoret. chim. Acta (Berl.) 23, 239—258 (1971)

Molecular Orbital Calculations of the Active Site Complex of Two Iron Ferredoxins

I. Energy-Conformation Studies

GILDA HARRIS LOEW and DAVID A. STEINBERG
Department of Genetics, Stanford University Medical Center, Stanford, California 94305

Received April 2, 1971

The results presented here are the first part of a systematic theoretical study of some of the physical and biochemical properties of two iron ferredoxins obtained by the use of an Extended Hückel Self-Consistent Charge iteration method of molecular orbital calculations. In this initial study, attention is focused on the calculation of electronic energies as a function of molecular geometry and the nature of the bonding ligands at the active site in order to determine the most stable form of the active site complex. Included in the active site complex are two iron atoms, two acid labile sulfur atoms of unknown inorganic origin and four sulfur atoms presumably from nearby cysteine residues. Fifteen chemical-conformational variations of this basic active site complex were considered. Among these conformational variations of the sulfur ligands, Fe–Fe distances, bond lengths and angles and chemical variations such as the effect of axial ligands, disulfide bonds and added protons were included. Our results indicate that that with all reasonable variations of the ligands, the preferred molecular geometry about 4-coordinated Fe is tetrahedral rather than planar. The planar conformation is somewhat stabilized by the addition of axial ligands, but is still less favorable than the tetrahedral conformation. In this model, interactions between the two iron atoms occur automatically since they are both part of the same active site complex. Hence the absence of low temperature paramagnetism in the oxidized state is readily explained. Preliminary investigations of the reduced state with one additional electron indicate that the odd electron is delocalized, as observed in both ESR and ENDOR. Its presence apparently substantially destabilizes all of the molecular orbital energies in accord with the observation that only one electron can be added to these proteins without decomposing them.

Die vorliegenden Ergebnisse stellen den ersten Teil einer systematischen theoretischen Untersuchung einiger physikalischer und biochemischer Eigenschaften des Fe_2-Ferredoxins mit Hilfe einer selbstkonsistenten erweiterten Hückelmethode dar. In diesem ersten Teil wird besonders die elektronische Energie in Abhängigkeit von der Molekülgeometrie und der Art der Liganden an der aktiven Stelle untersucht, um die stabilste Form des Komplexes der aktiven Stelle zu finden. Dieser Komplex enthält zwei Eisenatome, zwei saure, nicht fest gebundene Schwefelatome unbekannter anorganischer Herkunft sowie vier Schwefelatome, vermutlich aus nahegelegenen Cysteinresten. Bei den 15 untersuchten Konformationen der Schwefelliganden wurden Änderungen der Fe–Fe-Abstände, Bindungslängen und -winkel sowie chemische Variationen wie die Einwirkung der axialen Liganden, der Disulfidbindungen und zusätzlicher Protonen berücksichtigt. Es ergibt sich, daß das Eisen vierfach tetraedrisch koordiniert ist und nicht planar, selbst bei der Addition axialer Liganden. In diesem Modell ergeben sich Wechselwirkungen zwischen den beiden Eisenatomen zwanglos, da sie zum gleichen aktiven Komplex gehören. Dadurch wird das Fehlen eines Tieftemperatur-Paramagnetismus im oxydierten Zustand hinreichend erklärt. Eine vorläufige Untersuchung des reduzierten Zustandes mit einem zusätzlichen Elektron zeigt, daß dieses delokalisiert ist, genau wie es mit ESR und ENDOR beobachtet wird. Seine Gegenwart destabilisiert offenbar alle MO-Energien, was in Übereinstimmung mit der Beobachtung steht, daß nur ein Elektron von diesen Proteinen addiert werden kann, ohne sie zu zerstören.

1. Introduction and Background

The iron-sulfur, nonheme proteins, now called "plant type" ferredoxins [1] contain two iron and two labile sulfur atoms [2, 3]. Members of this group of proteins are of plant origin such as spinach and parsley, animal origin such as adrenodoxin and bacterial origin (proteins are of the same origin) such as putidaredoxin, and proteins I and II from azobacteria. They participate in a wide variety of biological processes such as photosynthesis, nitrogen fixation, hydroxylation of terpenes and steroids and are in the mitochondria respiratory chain. In most instances they serve as electron transfer agents by reversible oxidation reduction. Surprisingly, reductive titration experiments [4, 5, 6] have shown that these two-iron proteins can only take up one electron reversibly, being unstable to the addition of a second electron. Both electron spin resonance (ESR) [7, 8, 9) and electron, nuclear double spin resonance, ENDOR [9] experiments for a number of these proteins clearly implicate both iron atoms in this one electron uptake. Additional evidence for the interaction of the two iron atoms at the active site is the observed low temperature diamagnetism [10] of the oxidized state of these proteins. The two iron atoms may hence be considered to be at the center of the active site for electron transfer. In addition ESR experiments have clearly indicated that the added electron has some density on both the labile sulfur atoms [7, 11, 12, 13, 14] and the sulfur atoms of at least four cysteine residues in the vicinity of the iron atoms [15]. Linear sequencing of a number of these two-iron ferredoxins [16, 17, 18, 19] also indicates the possibility of four cysteine residues in the vicinity of the iron atoms. In all of these proteins then two iron atoms, two labile sulfur atoms and four sulfur atoms of cysteine residues are assumed to be part of an active site complex as shown in Fig. 1. In this complex, each Fe atom is thought to be coordinated to four sulfur ligands, two labile sulfur atoms acting as a bridge between the irons and two from the cysteine residues.

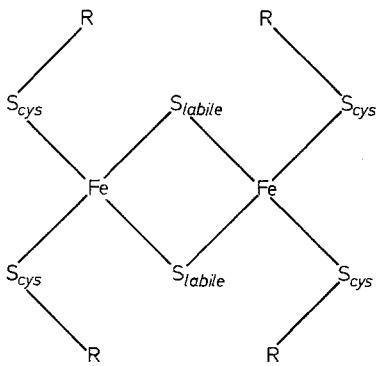

Fig. 1. General molecular model of active site complex of two-iron ferredoxins

While the involvement of the iron and sulfur atoms at the active site as shown in Fig. 1 has been fairly well established, important conformational and chemical information is still lacking. Unlike heme proteins, this active site complex is not a separable entity. Attempts to prepare the apoprotein result only in the removal

of two iron atoms and the two acid labile sulfur atoms usually in the form of H_2S [7, 20, 21, 22, 23]. Nor has the three dimensional structure of any of these two iron proteins been determined by X-ray diffraction as has been done for the one iron ferredoxins, called rubredoxins [24]. Difficulty in growing large enough crystals seems to be impeding the progress in such investigations [25]. Thus the active site complex apparently common to all plant type ferredoxins, with small variations, is more difficult to characterize than in heme proteins. For example, the observed g value in ESR spectra [21], the anisotropic hyperfine coupling constant in ENDOR [9], and the optical activity of circular dichroism [27] establish some sort of rhombic symmetry, that is the inequivalence of the three axial directions about the Fe ion in most of the two iron ferredoxins. However, the arrangement of the ligand atoms causing this rhombicity is not known. Also unknown is the detailed chemical nature of the ligands and therefore of the iron itself.

In spite of the rather self-evident molecular aspects of the active site complex, such as the proximity of the atoms, electron pairing and electron delocalization, all attempts to explain the experimentally observed properties of these proteins have been based on the use of the localized crystal field model for the active site. The use of this model presumes two independent iron atoms each perturbed by an electrostatic field caused by a regular array of ligand atoms. Both tetrahedral and square planar arrangements of the sulfur atoms about each iron atom have been proposed [28, 29, 30] but neither experimental nor theoretical analysis based on the crystal field formalism have established the validity of either. Crystal field models do not specify the ligand explicity and must make an a priori assumption of the formal valence and spin state of the iron. For example descriptions of the active site of the two iron ferredoxins in this format have been attempted in terms of ferrous and ferric ions in high or low spin states in the two redox forms [28, 29, 30, 47]. In these descriptions, experimental properties, particularly the g values from the ESR spectra of the reduced state and the electronic spectra have been used to deduce the nature of the perturbed d orbital states of the two Fe ions rather than the reverse process. Thus, even within the crystal field framework no bona fide calculation of the perturbed energies and states of the two iron atoms have been attempted.

Oxidized	Reduced	Explains	Ref.
1. $Fe^{+2}(1s) - Fe^{+2}(1s)$	$Fe^{+2}(1s) - Fe^{+1}(1s)$	1, 3 not 2	[47]
2. $Fe^{+2}\begin{pmatrix} hs \\ 1s \end{pmatrix} - Fe^{+3}\begin{pmatrix} hs \\ 1s \end{pmatrix}$	$Fe^{+2}\begin{pmatrix} hs \\ 1s \end{pmatrix} Fe^{+2}\begin{pmatrix} hs \\ 1s \end{pmatrix}$	2 not 1, 3	
3. $Fe^{+3}(1s) - Fe^{+3}(1s)$	$Fe^{+2}(1s) - Fe^{+3}(1s)$	3 not 1, 2	[30, 47]
4. $Fe^{+3}(hs) - Fe^{+3}(hs)$	$Fe^{+2}(hs) - Fe^{+3}(hs)$	None	[28, 29]

Additionally, the inherent limitations of this formalism do not allow even a qualitative description of a number of important physical properties which appear primarily to be the result of electron delocalization and bonding interactions of a

molecular species. Such properties are: 1. the low-temperature diamagnetism of the oxidized state; 2. the limited one-electron reduction; and 3. the single, delocalized unpaired electron spin in the reduced state. Given below is a list of four combinations of valence and spin states of the 2 Fe atoms which have been proposed as a basis for the crystal field perturbation indicating which of these properties are explained, by each choice.

It is apparent from this table that there is not one combination of independent ions that simultaneously explains all three properties, even if the additional observed feature of delocalization is disregarded. In an attempt to ameliorate this defect, an antiferromagnetic exchange interaction between the 2 Fe atoms in the oxidized state has been proposed [28]. Again, as with the crystal field perturbation itself, the proposal has been in the form of a phenomenological description with no calculation of the interaction reported. For example, possibilities (3) and (4) have both been considered with two ferric ions in high or low spin states strongly perturbed by their nearest neighbor and independent except for this antiferromagnetic coupling which leaves their spins paired. Without any mathematical formulation of this interaction, it is then necessary to accept on faith alone this explanation of the observed spin pairing.

A further indication of the difficulties inherent in the proposal of an antiferromagnetic exchange interaction, is the observance of room temperature paramagnetism [28, 43] of the oxidized state. Susceptibility measurements indicate the onset of paramagnetism at about 100° K, [10] a temperature much higher than the usual antiferromagnetic-paramagnetic transition temperatures. Since the transition temperature is directly related to the antiferromagnetic exchange energy, a bona fide calculation of the exchange interaction should explain both the low temperature diamagnetism and the onset of paramagnetism. In such a case, this model would gain considerable credence, at least for the oxidized state where the manifestations of electron delocalization are not as apparent. But lacking such a calculation, acceptance of the exchange assumption is tantamount to solving the problem by definition which yields little of heuristic value.

Similar difficulties are encountered with this model in attempts to explain the one electron reduction as localized on one of the Fe atoms. Since these Fe atoms are known to be equivalent in the oxidized state [42], it is difficult to explain why both are not reduced. ESR and ENDOR spectra both indicate delocalization of the unpaired spin density on both iron atoms as well as the sulfur ligands in the reduced state. Such a delocalization is incompatible with two independent Fe ions in a crystal field. In discussions of the crystal field models, delocalization has been mentioned [28] as a possible way out of this dilemma but no calculation of it or its consequences for limited reduction have been made.

Thus all attempts to describe the reduced state share the notion of two independent Fe ions, one of which has been reduced. In the Brintzinger *et al.* model [30] both ferrous and ferric ions are assumed to be in the low spin state. This model eliminates the necessity for considering an exchange interaction to account for a single unpaired spin. However, the added electron is localized on one Fe ion while the spin density is localized on the other, in direct contradiction with observed properties. There is moreover no reason offered why the second ferric ion cannot be reduced. In fact one would predict this result. With this model, no observed

properties are calculated, but rather g-values are used to further elucidate the nature of the perturbed ferric ion states assumed from the spectra to be relevant.

In the other prevalent model of the reduced state of Whatley *et al.* [28, 29] both ferrous and ferric ions are assumed to be high spin. An antiferromagnetic exchange interaction is again invoked this time to account for the appearance of only one unpaired spin. Once more no calculation of this interaction is presented. Additionally, the delocalization of this unpaired electron is assumed, with no elaboration, to account for the single reduction. Neither the delocalization nor the exchange interaction is calculated, nor are any other properties of the system. Instead, g-values are again used to deduce the nature of the perturbed ionic orbitals. Thus g-values have been equally well "explained" with and without antiferromagnetic exchange.

In the Whatley model [28] an order of magnitude estimate is made of the expected isotropic Fe^{57}-unpaired spin coupling constant (A-values) for a coupled ferrous and ferric ion. In this estimate, individual A values are not calculated. Instead two values are assumed and used in a coupled expression for the total A value. The results are meant as a plausibility argument for the model of antiferromagnetically coupled high spin ferric and ferrous ions in the reduced state. Since no bona fide calculations of any observed properties of the reduced state have been made with either model, and given the conceptual difficulties we have been discussing, the validity of both is open to question. While these pioneering efforts have begun to elucidate some aspects of the active site, the inherent limitations of the crystal field model mitigated, in our estimation, against using it for more quantitative calculations of the properties of the active site.

In order then to further elucidate the conformational and chemical nature of the active site complex, we have made molecular orbital calculations for several plausible molecular models. In these studies, we have included the two iron atoms and six sulfur atoms of the basic complex shown in Fig. 1, and have varied both the atomic participants in the active site complex and their conformations. For each molecular conformer chosen we have calculated a number of configuration energies to determine the lowest energy configuration as well as the minimum energy conformations. For these calculations, we have used the so-called Extended Hückel Self Consistent Charge method which has been used to study iron-heme complexes [31–32] among other frequent applications. The results of such semi-empirical calculations give configuration energies and reasonable electron distributions in the molecule. From these a number of other electronic properties of interest can be calculated. In this initial report we wish to primarily discuss the insight into the nature of the active site complex which our energy conformation studies afford. In addition, we show how such important properties as the observed magnetic moment behavior of the oxidized state and the limited single electron reduction involving both iron atoms can be explained on the basis of the results of our calculations. Finally we also present a preliminary study of the reduced state including the elucidation of the nature of the single unpaired electron. In subsequent reports we shall pursue this molecular orbital description and discuss in more detail the electronic properties of the most stable conformations of the active site complex.

2. Molecular Models

In any molecular orbital calculation, it is obviously necessary to first choose a molecular form from which the most physically meaningful results can be extracted. For the active site of proteins, particularly when they are not a prosthetic group or identified by X-ray analysis, this choice is not at all a trivial matter. In fact the purpose of this study is to help choose among several plausible models at least sufficiently to decide some of the salient characteristics of the active site complex. As was indicated in section I very little is known about the actual structure and composition of the Fe–S active site complex in the two iron ferredoxins. The bond lengths, bond angles, symmetry and even the number of atoms involved are all parameters whose variation is not very stringently determined by existing physical evidence. Hence we have chosen various combinations that seem to correspond to both what is known of the active site and the structural data of better known complexes. The X-ray crystallographic structure determination of rubredoxin at 1.5 Å resolution [25] indicates that the single Fe atom is surrounded by a distorted tetrahedron of 4 cysteine sulfur atoms each of which is at a slightly different distance from the Fe. The Fe–S distances range from 2.14 to 2.38 Å and the four angles from 100 to 116°. We have used these distances and angles as a guide in our choices for the two iron ferredoxins.

In the first model of the active site studied, we have, for the sake of simplicity, replaced the cystein *R* groups (really C_2H_5) by H atoms. For this molecule we have considered 6 different plausible conformations as shown in Fig. 2 and the table accompanying this figure. In this table we list all the relevant angles and distances, for each conformation. Forms $A - D$ involve essentially tetrahedral arrangements of the sulfur ligands about each Fe atom, with the S_b–Fe–S_b plane perpendicular to the plane of the rest of the molecule. In form *E* all the Fe and S atoms are in the same plane while in form *F*, the planar arrangement of the S atoms is retained but the Fe atoms are each raised out of the plane by .5 Å as they are in some iron-heme complexes [31]. In the two planar conformations, the arrangement of the S atoms about each Fe has rhombic character in keeping with most of the observed properties indicated above. Among the four tetrahedral conformations, small variations are further considered.

In forms *A* and *B* all the S atoms are conformationally equilvalent forming a regular tetrahedron about each Fe with bond lengths 2.3 Å and bond angles 109.5°. The resultant Fe–Fe distance is 2.65 Å. Form *A* and *B* differ only in the relative conformation of the "cysteine residue" here simulated by the H atoms. In conformation *A* there is a linear arrangement of the Fe–S_c–H atoms. In form *B* the more normal bond angle of 95.5 is used for divalent sulfur. In form *C* the tetrahedron about each Fe is distorted by making the cysteine sulfur atoms different from the bridge S atoms. The S_b–Fe–S_b angle is closed down to 90° relieving some of the strain in the 4 membered ring, and the Fe–S_b distance reduced to 2.10 Å. The resulting Fe–Fe distance is increased to 2.97 Å. Finally in form *D*, the two Fe sites are made somewhat inequivalent. Evidence of such inequivalence has been detected in the reduced state of the protein by both by ENDOR experiments which indicate different degrees of interaction of the unpaired electron spin with the two Fe^{57} nuclei, substituted for native Fe^{56} [9] and in Mössbauer Resonance experiments where the electric field gradient at the two Fe^{57} nuclei appears to be

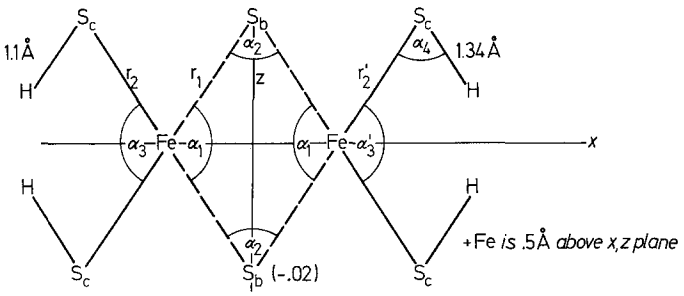

Geometry \ Form	$A(\pi_D)$	$B(T_D)$	$C(T_D)$	$D(T_D)$	$E(D_2)$	$F(C_{2v})^+$
α_1	109.5	109.5	90	109.5	90	90
α_2	70.5	70.5	90	70.5	90	90
α_3	109.5	109.5	109.5	120	109.5	109.5
α'_3	109.5	109.5	109.5	100	109.5	109.5
α_4	180	95.5	95.5	95.5	95.5	95.5
r_1	2.30	2.30	2.10	2.30	2.30	2.30
r_2	2.30	2.30	2.30	2.40	2.30	2.30
r'_2	2.30	2.30	2.30	2.20	2.30	2.30
r(Fe–Fe)	2.65	2.65	2.97	2.65	3.26	3.18
$r(S_b–S_b)$	3.76	3.76	2.97	3.76	3.26	3.26
Energy	−769.58	−775.77	−780.94	−771.31	−763.14	−761.90

Fig. 2. Model I series for active site complex of two-iron ferredoxins. Geometric parameters for 6 different conformations

different [42]. However, the origin of this inequivalence has not been explained. It must of course be related to the conformational or chemical differences in the environment about each Fe. Model *D* was designed to explore one such plausible conformational difference. As seen from Fig. 2 and the table in this model, each Fe has a slightly different relationship to its nearby cysteine S ligands. At one site the S_c–Fe–S_c bond angle is 100° and the Fe–S_c distance is 2.4 Å while at the other site the angle is 120° and the distance 2.2 Å. These variations are similar to the differences observed for Fe–S_c bonding in rubredoxin. The formal charge on the Fe derives from the formal charge that one assumes on each ligand and the overall charge of the complex. Thus, in this model, if each labile S ligand is an $S^=$ species and the cysteine sulfurs are HS^- then, for a neutral complex, the formal charge on each Fe is +IV. However, in a molecular orbital calculation one need not specify atomic charges. As we have already indicated they are the result of such calculations and never correspond to the formal charge picture. In this model there are 56 valence electrons and 46 valence atomic orbitals all of which are included in the calculation. For the totally paired configuration then, 28 orbitals are occupied and 18 are empty. Other configurations are made by considering promotions from filled to empty orbitals.

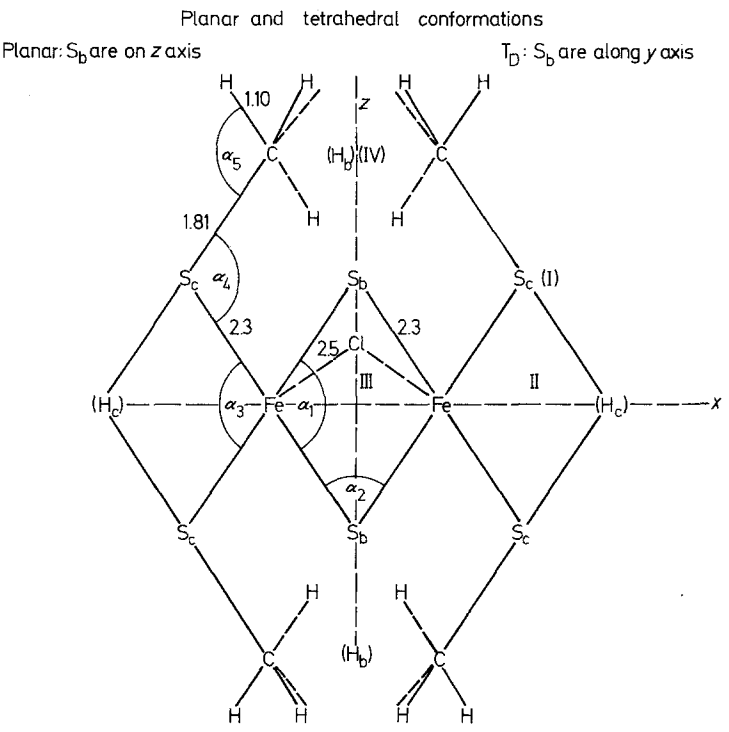

Fig. 3. Model II series for active site complex. Nine different chemical and conformational variations. Description given in Table 1

In a second model, we have replaced the H atoms of the cysteine S by CH_3 groups for a more realistic simulation of the cysteine residues, to re-enforce the conclusions drawn from the simpler model, to see if the electron density on the Fe and S atoms is changed appreciably, and to further our exploration of chemical-conformational variations of the active site complex. With this basic change then, 9 different chemical and conformational variations were considered. These are indicated in Fig. 3 and the accompanying Table 1.

Fig. 3 depicts all the variations and also gives the distances used in common. In the accompanying Table 1, is given for each form, the angles used, the Fe–Fe and S–S distances, the formal charge on the Fe, the nature of the ligands, and the number of valence electrons and the atomic orbitals in the molecular system. The relative orientation of the added CH_3 group on the S_c atoms was kept constant in all 9 variations. Tetrahedral symmetry about the methyl C was used with the H–C–S atoms in the S_c–Fe–S_c plane and the two other methyl hydrogens above and below the plane in regular tetrahedral arrangements. A value of 90° was used for the C–S_c–Fe angle in all of these forms.

In the first molecular model of this series (*A*) no other atoms were added to the complex. Four different conformations were considered. Conformation A_1 is a regular tetrahedral arrangement of all the S atoms about each Fe, identical to conformation *B* of the first, simpler series. Conformations A_3 and A_4 were chosen to explore the possible formation of disulfide bonds $S_2^=$ between either

Table 1. *Conformation, nature and energies for model II series of active site*

	A				B		C		D
Fe Ox #	+4		+3	+3	+3		+3		+4
Nature of S_b	$S^=$		$S^=$	$S_2^=$	$S^=$		$(H_bS_b)^-$		$S^=$
Nature of S_c	RS^-		$(RS_c)_2^-$	RS_b^-	S_c–H_c–S_c		RS^-		S_c–H_c–S_c
Axial ligand	none		none	none	none		none		$2Cl^-$
	$T_D(A_1)$	$D_2(A_2)$	$T_D(A_3)$	$T_D(A_4)$	$T_D(B_1)$	$D_2(B_2)$	$T_D(C_1)$	$D_2(C_2)$	$D_2(D_1)$
r(Fe–Fe)	2.66	3.26	3.26	4.20	2.66	3.26	2.66	3.26	3.26
α_1	109	90	90	45	109	90	109	90	90
α_2	71	90	90	135	71	90	71	90	90
α_3	109	90	45	90	109	90	109	90	90
α_4	90	90	90	90	90	90	90	90	90
α_5	109	109	109	109	109	109	109	109	109
S_b–S_b	3.76	3.26	3.26	2.08	3.76	3.26	3.76	3.26	3.26
S_c–S_c	3.76	3.26	2.08	3.26	3.76	3.26	3.76	3.26	3.26
# electrons	80	80	80	80	82	82	82	82	96
# M.O.	70	70	70	70	72	72	72	72	82
E_T	−1178.2	−1156.6	−1099	−1183.5	−1155.4	−1139.6	−1213.6	−1137.3	−1434.6
B.E.	− 106.8	− 94.6	− 90.8	− 107.8	− 104.2	− 90.6	− 112.7	− 89.0	− 97.6

E_T = Configuration energy.
B.E. Binding energy = $E_T - \Sigma E_i$(atom).

the cysteine sulfur atoms as in ($A3$) or the bridge sulfur atoms as in ($A4$). In $A3$ then the S_c–S_c distance was set equal to 2.08, the most common disulfide bond distance in proteins, and the same distance was chosen for S_b–S_b in A_4. The result is a very distorted tetrahedral arrangements of the 4 S atoms about the two Fe atoms with some unusually small bond angles as shown in Table 1. Conformation A_2 is a square planar arrangement of the S atoms about the Fe atoms. The formal charge on the Fe in molecular model A is +IV but is reduced to +3 in conformations $A3$ and $A4$ because of the possibility of disulfide bond formation. There are 80 valence electrons in this molecular system which are allowed to interact and distribute over 70 possible atomic orbitals in the formation of molecular orbitals. The resultant charge distributions in the molecule have very little similarity with the formal charges.

In molecular model B of this series the presence of protons in the vicinity of the ionized cysteine residues was explored. As shown in Fig. 3, two protons were added in positions for each to be shared symmetrically by two neighboring S_c atoms, thus reducing the formal charge on the Fe atoms to +3. Both a tetrahedral ($B1$) and square planar ($B2$) conformation were considered for this molecular system which has 82 valence electrons and 72 atomic orbitals.

In molecular model C of this series, the possibility that the labile bridge sulfur atoms are more like HS^- species was considered by the addition of an H atom to each of the bridge S atoms. Again, for this 82 electron, 72 orbital system, both a tetrahedral ($C1$) and a planar arrangement ($C2$) of the S atoms was considered.

Finally in model D, six coordination of the Fe atoms was considered by adding 2 Cl-ions as axial ligands in a bridge fashion, as shown in Fig. 3. There are 96 valence electrons and 82 atomic orbitals in this system. In this model all the S atoms are in a square planar arrangement, considered the most reasonable for six coordinated Fe.

Such then are the 15 different chemical-conformation variations we have considered for the active site of two-iron ferredoxins. The overall molecular symmetry of every active site model chosen is D_{2h} for both tetrahedral and planar arrangements of the S atoms about each Fe. Small deviations from this symmetry occur for the cases when the two Fe atoms are placed in inequivalent sites or lifted out of the plane of the S atoms. Thus, unlike one-transition metal complexes, the molecular symmetry can be quite different from that of the local environment of each ion which is the one considered in crystal field models. It is this overall symmetry which determines the way in which the atomic orbitals combine to form molecular orbitals. Thus for 2 iron complexes the nature of each mo and the corresponding electron distribution and energy levels resulting from our mo calculation has qualitatively different symmetry-determined attributes than those from the crystal or ligand field model. The effect of overall symmetry is manifest in many different properties for example the determination of allowed transitions in electronic spectra and the participation of non-bonding but symmetry equivalent atoms in the same molecular orbitals.

3. Method of Calculation

For such large molecular systems as the active site complex, it is not yet feasible to use *ab initio* SCF molecular orbital calculations. For our study then we have utilized a computer program based on a semi-empirical, one electron method

called the Extended Hückel Self-Consistent Charge iteration (EH–SCC) method. A simpler version of this method without charge iteration was first used to describe transition metal complexes [33] and has since received wide application, for example to study purines and pyrimidines [34], carbonium ions [35] and methylen. compounds [36]. As we have already mentioned, in its present form it has been used to study metal porphyrin compounds [31, 32]. Hence the details of this method have already been described and we shall give only its salient features.

In our calculation all valence electrons are allowed to interact in the nuclear framework chosen. All valence atomic orbitals are included in the calculation. For the six variations of Model I, there are 56 valence electrons and 46 atomic orbitals. For the nine variations of model II the number of electrons ranges from 80 to 96 and the number of valence atomic orbitals from 70 to 82. Each atomic orbital is represented by a single Slater type function of the form.

$$\chi(n, l, m) = Nr^{n-l}\exp(-\zeta r)\, Y_l^m(\Theta, \Phi). \tag{1}$$

The exponential factors used for each atomic orbital are taken from the best atomic calculations [31, 37]. Overlap integrals between all pairs of atomic orbitals are calculated. However, only one electron energy matrix elements H_{pp} and H_{pq} are evaluated. These are empirically determined from the valence state ionization potential of each atomic orbital which is used for the daigonal matrix elements. The off-diagonal elements are given by the expression:

$$H_{pq} = (1/2)\,(H_{pp} + H_{qq}) \cdot S_{pq}[\chi + (1-\chi)\, S_{pq}] \tag{2}$$

where S_{pq} is the overlap between atomic orbitals p and q and χ is their interaction parameter taken in these calculations to be 1.89, as in the iron-porphyrin calculations [31, 37]. Input to the program involves specifying the molecular geometry, i.e. the coordinates of each atom, the orbital exponential factors, an initial guess as to the charge on each atom which is usually taken to be zero or a very small fraction of a unit charge and the valence state ionization potential of each atomic orbital. In the charge iteration procedure, these ionization potentials are a linear function of the charge on each atom. With this variation, the program iteratively calculates the energy eigenfunctions and eigenvalues, which correspond to a self-consistent value of the net charge on each atom, one in which the input and output values of the charges agree to a specified tolerance. The net charge on each atom is obtained after each matrix diagonalization from a Mulliken population analysis [38] of the resulting charge distribution. The charge iteration feature of these calculations allow a reasonable charge distribution to be obtained as manifest for example in frequent agreement between measured and calculated values of dipole moments. The net atomic charges calculated are very much smaller than the formal charge associated with atoms in molecules and rarely approach a unit charge.

The electron distribution in the molecule is obtained as a set of N molecular orbitals, which are linear combinations of the original N atomic orbitals (LCAO) X_j:

$$\psi_i = \sum_{J=1}^{N} C_{ij} X_j\,. \tag{3}$$

These molecular orbitals are eigenfunctions of the one-electron effective Hamiltonian which characterizes the Extended Hückel method of solution of the Schroedinger Equation. In addition, they are also eigenfunctions of the symmetry operations of the D_{2h} point group of the molecule, each belonging to an irreducible representation of that group. The atomic orbitals contribute to each molecular orbital in such a way as to form these symmetry eigenfunctions, with symmetry equivalent atoms appearing as partners in the molecular orbitals. For example, the two Fe atoms participate in molecular orbitals using identical pairs of appropriate atomic orbitals. If the two atoms are totally equivalent, these pairs enter with the same numerical coefficient. Inequivalence is manifest in somewhat different coefficients for the parts of atomic orbitals in a given molecular orbital. In either case the two Fe atoms form plus and minus combinations $(X_i \pm X_i)$ of identical atomic orbitals which allow them to participate in both odd (u) and even (g) molecular orbitals. This behavior is unlike the situation for one metal ion complexes with a center of symmetry in which d orbitals participate only in even (g) orbitals and has a direct bearing on the analysis of the electronic spectra. Similar behavior is found for all other sets of symmetry equivalent or near-equivalent atoms at the active site complex. Thus, allowing all atomic orbitals to interact in a specified nuclear framework with a given symmetry results in a description of the electron distribution which can include Fe–Fe interaction and in general the delocalization of electrons in symmetry compatible atomic orbitals on all the atoms of the active site.

In addition to sets of molecular orbitals, a corresponding set of one-electron orbital energies are also obtained. Specifying the occupancy of the orbitals specifies a configuration of the molecule. The resulting valence configuration energy is then: $E_t = \sum_i n_i \varepsilon_i(mo)$ summed over all occupied orbitals.

Valence configuration energies are only a small part of the total energy of the molecule which can be written as the sum of four terms:

$$E = \sum_i^{\text{val}} n_i \varepsilon_i(mo) + \sum_j^{\text{core}} \varepsilon_j(mo) + E_{ee} + E_n$$

where the first term is the valence electron configuration energy, the second the core electron configuration energy and the third the electron correlation energy and the fourth the nuclear repulsion energy. The first three terms contribute to the stability of the molecule with the second and third being by far the largest contributions, while the last term is repulsive and partially cancels the effect of the other three, being of much larger magnitude than the first term alone. It is only the first and smallest part of the electronic energy which we calculate. Because of the semi-empirical nature of our calculation and because of the charge iteration procedure used, each orbital energy is not entirely independent of the number and nature of the filled orbitals i.e., there is some electron correlation built into the system. Thus for example, separate valence configuration energy calculations should be made for each configuration of interest rather than determining the value of this term for excited configurations by promotions from the most paired ones. Even with this refinement in the EHSCC method, we cannot hope to calculate realistic total energies, nor is this our aim. We mean simply to use the first term of the total energy, calculated semi-empirically, to determine the relative stabilities

of different conformations and configurations of a given molecular system. Fortunately, it has been proposed for quite some time [39] and more recently put on a sound general theoretical basis [41] and also with specific reference to the results of EH calculations [44, 45, 46] and EHSCC calculations [40] that the variation in valence configuration energy with molecular conformation parallels that of the total energy as determined by SCF calculations. Hence the energies that we calculate can be used with some degree of confidence to determine the relative stabilities of a series of different conformations of a given molecular system. This is the main use we shall make of the "total energies" E_t which we calculate.

To compare the relative stabilities of molecular models with different numbers of atoms and electrons, binding energies rather than total configuration energy differences must be used. These energies are defined as:

$$\text{B.E.} = E_t - \sum_{A}^{\text{atoms}} E_A$$

where E_t = total molecular energy, E_A = total energy of each atom in the molecule:

$$E_A = \sum_{i}^{\text{val}} n_i \varepsilon_i(\text{a.o.}) + \sum_{j}^{\text{core}} 2\varepsilon_j(\text{a.o.}) + E_{ee} \,.$$

As with the molecular energy, we calculate only the first and smallest term of the atomic energy expression, the valence electron energy, for each atom. Our approximate calculation of binding energies then consists of the subtraction of the sum of atomic valence configuration energies from the molecular one, i.e., in the above expression for B.E. only the first terms of both E_t and E_A are used.

In our previous analysis [40] we have shown that at least for the test case studied, binding energies calculated in this way from the results of EH–SCC methods, are of the same order of magnitude as those calculated by the more exact SCF molecular and atomic calculations and thar they agree as well with experimental values. For stability studies the use of binding energy differences are however not as reliable as the use of molecular configuration energies and are only used when differences in the number of atoms and electrons precludes an E_t comparison.

4. Results

A. Configuration Energies: Diamagnetic Ground State of Oxidized Active Site

For each of our 15 molecular models we have used our EHSCC molecular orbital program to calculate the configuration energy for the totally paired configuration. In no case was the highest filled orbital degenerate, indicating to this extent that the totally paired configuration is the lowest energy one. To more accurately test this result we made additional energy calculations for a number of excited configurations with 2 or more 1/2 filled orbitals. Again, by direct comparison of the calculated valence configuration energies, E_t, the totally paired configuration had the lowest energy. This result, at least in the one electron approximation, explains the observed low temperature diamagnetism of the

oxidized state of these two-iron proteins. We have thus explained one of the most puzzling aspects of the oxidized state of these two-iron proteins as the natural result of interactions among the atoms at the active site. This spin-pairing was not an assumption of our model, but rather a result of our calculation. Further, it is a property of the entire molecule and need not be attributed to local spin pairings at or between each Fe atom or any other atom in the molecule. In all of these ways then the explanation of the observed low temperature diamagnetism of the oxidized state is superior to the one previously discussed based on a crystal field model of the two-iron active site. As we have already discussed at some length in the introduction, this explanation involved the a priori choice of spin and oxidation states of zwo Fe atoms assumed to be independent but then postulated to be interacting through an antiferromagnetic exchange interaction. Moreover, the interaction was never calculated but simply presented as a suggestion for the observed magnetic behavior of the oxidized state, nor were any other properties of the oxidized state linked to its presence.

In addition to a totally paired ground state, there are in most molecular models considered a number of low lying biradical excited configurations within thermal energy range of the ground state. This characteristic of our model could then explain qualitatively the observed room temperature paramagnetism of the oxidized state of some of these proteins. Having thus determined an energy ordering of configurations within each conformation which corresponds to the observed magnetic behavior of the oxidized state of these two-iron proteins, we shall use the energies of totally paired configuration to compare the stabilities of the different chemical conformation studies.

B. Relative Stability of Active Site Conformations and Net Atomic Charges of Model I

For molecular model I of the active site, we have calculated the totally paired and excited configuration energies for the six conformations shown in Fig. 2. The final energies obtained after charge convergence are somewhat sensitive to the initial charges chosen and the degree of convergence of the charges on each atom. A set of consistent, totally-paired configuration from a well converged result is given in the last row of the table of Fig. 2. We see from the results in this table that the most favored conformation is *C*, a distorted tetrahedral arrangement of the two labile bridge sulfur atoms and two somewhat differently bonded cysteine sulfur atoms about two equivalent Fe atoms. This lowest energy conformation is very similar to the one described for rubredoxin from X-ray structure determination [25]. Preliminary results from ESR broadening due to S^{33} substituted for S^{32} in both labile and cysteine sulfur atoms [7, 15] also show some inequivalence of these two types of sulfur atoms in the reduced state.

Our results further indicate that this conformation is stable to both greater and smaller differences at the two Fe atom binding sites. On the one hand, the more regular tetrahedral arrangement, *B*, of the 4 S atoms about the Fe atoms in which the labile and cysteine sulfur atoms are all equivalent is less stable. On the other hand, distorting the tetrahedron further in such a way as to make the two pairs of cysteine sulfur atoms inequivalent and therefore the two Fe binding sites inequivalent, as in form *D*, also increases the energy. The destabilization is about

9.6 eV thus indicating that, at least in the oxidized state, equilvalent Fe sites are preferred. Mössbauer resonance results [42] in which only one quadrupole split doublet was seen in the oxidized state of 8 of these proteins appear to corroborate these results.

A linear cysteine S_c bond, i.e. R ... S_c ... Fe is very unfavorable, form *A* having the highest energy of all the tetrahedral conformations. This result indicates that the S atoms in the cysteine residues form normal divalent bonds.

Neither of the two planar structures are as stable as any of the tetrahedral arrangements just discussed. Moreover, raising the Fe out of the plane of the S atoms is less favorable than the totally planar conformation.

In all of the conformations of molecular model I, both Fe atoms have a formal charge of +IV stemming from the implicit nature of the attached ligands. However, in the molecular orbital calculations, as we have already mentioned, we have started with natural atoms and calculated the net charge on each atom from the iterated charge distributions, using a Mulliken population analysis [38]. The net atomic charges for each conformation are given in Table 2 and the accompanying figure displays the atoms and their formal charges. We see that, as is usually the case, there is a large difference between the formal and actual charge attributed to each atom and that there is no large charge build up on any one atom. All the atoms are almost neutral and the net charge is not a very sensitive function of the geometry.

To summarize then, our energy-conformation studies for model I of the active site complex indicate that the most favored conformation about each Fe is a distorted tetrahedron very similar to that about the single Fe in rubredoxin; that the Fe–Fe distance is about 2.97 Å; that the labile S atoms are bonded to the Fe differently from the cysteine S atoms, but that the two Fe atoms are in equilvalent sites. Tetrahedral arrangements of the 4 S atoms are preferred over planar ones,

Table 2. *Summary of ferredoxin atomic charges for 6 conformations of model I*

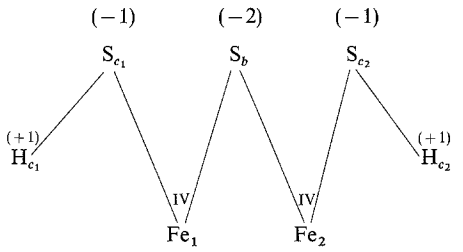

Atom \ Geometry	*A*	*B*	*C*	*D*	*E*	*F*
H_c	+.04	+.03	+.022	+.035 (+.046)	.037	+.037
S_c	−.10	−.08	−.104	−.092 (−.067)	.086	−.083
Fe	+.175	+.18	+.178	+.161 (+.168)	.145	+.143
S_b	−.06	−.07	−.01	−.087	−.044	−.048

(*n*) = charge on inequivalent partner in this geometry.

the cysteine S bonding is normal for divalent S and the charge on each atom is very small. These results offer a former basis for a choice of active site conformation than has hitherto been offered by the use of the crystal field formalism. In addition as indicated, they are partially corroborated by direct experimental evidence.

C. Relative Stabilities and Net Atomic Charges in Molecular Model II

Table 1 presents the energies of the totally paired configuration for the 9 variation tested with the cysteine hydrogen replaced by a methyl group. Several interesting further conclusions about the active site can be drawn from these results.

For the model A subset in which no other atoms but the CH_3 groups were added to the model I molecule, a tetrahedral arrangement of the S atoms was again the lowest energy form. Of the 3 tetrahedral arrangements considered, the distorted one A_4, in which disulfide bond formation is allowed between the two labile S atoms is the most stable. Both this form and the regular tetrahedral arrangement, A_1 are more stable than a planar arrangement of the S atoms, A_2. The conformation which allows disulfide bridges between the two cysteine S atoms A_3 appears to be the least stable.

For molecular systems B and C in which protons were added to the active site, the most stable arrangement of the S atoms in each case was again found to be tetrahedral ($B1$ and $C1$) rather than planar ($B2$ and $C2$). In addition comparing $B1$ and $C1$, it appears more favorable for the protons to be near the bridge S atoms than near the cysteine S atoms.

The six coordinate Fe complex D has the lowest configuration energy, but its stability cannot be directly compared to any other form, because of the increased number of atoms and electrons in this system.

To compare the relative stability of molecular models with differing numbers of atoms and electrons, as was previously mentioned, binding energies rather than total configuration energies were used. They are also given in Table 1, for the nine variations studied. These energies are not in general as reliable a criterion for considering relative stabilities as are the E_t values, but they are the only ones that can be used to compare systems which differ in the number of atoms and electrons. We are somewhat heartened in our use of them by noting that the relative ordering of the conformations with the same number of atoms and electrons does not change when the binding energy criteria is applied. Using the binding energies to compare the stability of all nine variations studied, then, the following general picture emerges. For all molecular models chosen a tetrahedral arrangement of the 4 S atoms about each Fe is preferred over a planar one. However, a planar arrangement of the S atoms is stabilized if the Fe is six-coordinated for example with Cl^- as an axial ligand. The most stable chemical-conformation model of all is $C1$ with a tetrahedral arrangement of the S atoms and the bridge S atoms as HS_b^- ligands. The next most favorable conformation appears to be tetrahedral form $A4$ with disulfide bonds between the bridge S atoms, and the Fe–Fe distance increased to 4.20 Å over the 2.65 Å in model $C1$. In both forms, the formal charge on the Fe is $+3$, the formal charge on the S_b is reduced and the S_b and S_c ligands are inequivalent.

Table 3. *Summary of atomic charges model II series of active site of ferredoxins*

Atom \ Model	A_1	A_2	A_4	B_1	B_2	C_1	C_2	D_1
Fe	+.12	+.02	+.114	+.08	+.02	+.095	+.055	+.063
S_b	−.136	+.06	+.025	−.08	−.06	−.06	−.11	+.15
S_c	−.085	−.26	−.094	−.007	−.16	−.12	−.16	−.13
H_c	—	—	—	+.04	−.04	—	—	−.107
H_b	—	—	—	—	—	−.06	+.21	—
Cl	—	—	—	—	—	—	—	−.468
C_m	−.20	−.16	−.193	−.12	−.067	−.11	−.098	−.10
H_m[a]	−.08	+.13	+.08	+.08	+.09	+.07	+.04	+.13
H'_m[a]	+.11	+.13	+.07	+.09	+.09	+.07	+.07	+.14

[a] H_m, H'_m are in plane and out of plane H atoms respectively.

The net charge obtained on each atom at the active site of all nine variations is given in Table 3. Again, as in the simpler model, there is very little charge build up on any of the atoms, and none resemble their formal charge. The differences in net atomic charges between the +3 and +4 forms are no larger than the small variations within each group. In spite of this similarity, the results of this calculation seem to indicate that an active site complex in which the Fe has a formal +3 charge is preferred over those in which it is +4 and that a corresponding reduction in the bridge sulfur formal charge is preferred over one on the cysteine S atoms.

D. Composite Picture of the Active Site Complex in Oxidized Two Iron Ferredoxins

The totality of the stability studies presented here, albeit obtained from the use of a semi-empirical, one electron molecule orbital calculation, allow substantial additional insight into the nature of the active site complex in the two iron ferredoxins. The results of our calculations indicate:

1. The two Fe atoms are each surrounded by a somewhat distorted tetrahedron of sulfur atoms.
2. The two Fe sites are equivalent, but the bridge S atoms bind to the Fe atoms differently than the cysteine S atoms.
3. Six-coordination of the Fe atoms stabilizes a planar arrangement of the S atoms but not sufficiently to compete with the four coordinated tetrahedral arrangement.
4. The preferred *formal* charge in the Fe atoms is +3 rather than +4.
5. The labile S atoms do not appear to be $S^=$ ligands but rather some species such as HS^- or $S_2^=$ with reduced formal charge.
6. The cysteine S atoms appear to have normal divalent bonding.
7. The electrons are distributed in such a way as to cause only a small positive charge on the Fe atoms and a small negative charge on the sulfur atoms, very different from their formal charge.
8. The lowest energy configuration is one in which there are no unpaired electrons, but there are a large number of low lying empty orbitals. Typically, the energy separation between the highest filled and lowest empty orbital is about

.02 eV corresponding to room temperature thermal energies. These results then can account for both the low temperature diamagnetism [10] and the observed room temperature paramagnetism [43, 30] by thermal population of excited states.

E. Preliminary Study of the Reduced State of the Active Site Complex

In the reduced state the two Fe sites appear to be inequivalent, judging from both ENDOR [9] and Mössbauer resonance [42] results involving substitution of Fe^{57} into the proteins. This the combined processes of reduction and isotope substitution cause a chemical-conformation change of unknown origin in the active site complex. Hence, we have begun a systematic exploration of plausible reduced state conformations in the same spirit of the study just presented. It does not seem likely that there are cross changes in the environment upon reduction nor are they necessary to account for both differences in quadrupole splitting [42] and electron-nuclear spin interactions [9]. Conformation *D* of model I is an example of a possible inequivalence.

Before embarking on our systematic analysis, and because we expect only small changes to occur, we have made a trial calculation for one reduced state obtained simply by the addition of one more electron to the most stable conformation of the oxidized state form *C* of model I. We wished ascertain whether, from the electronic distributions and energies calculated for the reduced state, we could account for some of its salient features; for example, the fact that a second electron cannot be added to this reduced state and the observed delocalization of the added electron on the Fe and S atoms at the active site. We have therefore made a charge iteration calculation for conformation *C* with 57 electrons in several configurations. Our results indicate that the lowest energy configuration of the reduced state is one in which there is only one unpaired electron, corresponding to the observed intensity of the ESR signal [5, 7]. The unpaired electron is in the 29th orbital which is empty in the oxidized state. In Table 4 we present some of the main properties calculated for the reduced state system. These include the total configuration energy, E_t, the promotion energy ΔE of an electron from the 28 to the 29th orbital, the energy of the 1/2 filled orbital, and the electron distribution in that orbital. Also in this table, we present these same quantities for the oxidized state in which the 29th orbital is empty. Several interesting conclusions can be drawn from the results in this table.

Table 4. *Preliminary exploration of reduced ferredoxin oxidized and reduced state of model IC*

State	E_t[a]	ΔE[b]	E_{29}[c]	Net atomic charge				Unpaired spin density/atom[d]			
				S_c	S_b	Fe	H	$S_c(p_y)$	$S_b(p_x)$	$Fe(d_{xy})$	$H_c(1s)$
Oxidized	−780.9	.07	−10.10	−.104	−.008	+.178	+.02	.10	0.6	.25	0
Reduced	−755.9	.06	− 9.53	−.210	−.130	+.080	−.10	.085	.070	.27	0

[a] E_t = Configuration energy for most paired configuration, all energies in eV.
[b] ΔE = Promotion energy from filled orbital 28 to empty or $\frac{1}{2}$ empty orbital 29.
[c] E_{29} = Energy of 29th orbital.
[d] In oxydized state this orbital is empty, in reduced state it has 1 electron so that: $2Fe(d_{xy}) + 4S_c(p_y) + 2S_b(p_x) + 4H_c(s) = 1$.

From the promotion energy we see that the lowest empty orbital of the oxidized form is only .07 eV above the highest filled one and that it has an energy of -10.1 eV. This value then is a zero order estimate of the electron affinity of the oxidized state of the protein. However, we have used the more accurate way to assess the effect of an added electron on the oxidized state, by repeating the entire self-consistent charge calculation for the 57 electron system. As we have already discussed, this method introduces some electron correlation energy. We see the effect of this electron correlation in the results in Table 4 for the reduced state. The energy of orbital 29 into which the electron is placed is changed somewhat from its value when it was empty. But more dramatically, through the charge iteration process, this added electron somewhat destabilizes the energy of all the filled molecular orbitals so that the result is a large total energy difference between the oxidized and reduced state. As seen from Table 4, the difference in the E_t values is 25 eV, more than twice the energy of the additional filled orbital. So large an energy difference for the reaction: 2 Fe(ox) $\xrightarrow{1e^-}$ 2 Fe(red) can account for the difficulty in adding still another electron to the system.

The population analysis of the electron distribution in the oxidized and reduced states, as seen from Table 4, indicates the added charge is distributed on all the Fe and S atoms. Each cysteine S increases its negative charge from .1 to .2 of an electron, while the bridge S are reduced from almost neutral to $-.13$. The charge on the iron atoms is reduced by half and the H atoms acquire a small negative charge. The added electron density on each atom does not come entirely from the unpaired electron in the highest filled orbital but also is the result of a slight redistribution of electron density in all the filled molecular orbitals.

Table 4 also gives the electron distribution of the unpaired electron, the so-called spin density, in the reduced state and also the nature of the same orbital when empty in the oxidized state. As shown in this table it is delocalized d_{xy} orbital in both cases with somewhat different electron distribution. In the reduced state the orbital has 54% *d* character equally distributed on each Fe atom and is delocalized with 8.5% density in the P_y orbital of each cysteine S atom and 7% on each labile S atom in a P_x orbital. These preliminary results then offer a qualitative explanation of the observed hyperfine broadening in the ESR of the reduced spectra with S^{33} substituted for both labile and cysteine S atoms. Encouraged by this initial success, a more systematic study of various models for the reduced state is now in progress, and a more detailed and quantitative description will be presented in a future paper.

Acknowledgement. The authors wish to gratefully acknowledge the support of NSF grant GB 17980 for this work. They also wish to thank Drs. Orme-Johnson, Graham Palmer, John Tsibris and Helmut Beinert for many helpful discussions.

Bibliography

1. Beinert, H.: In: Mössbauer resonance in biological systems. Ed. by Debrunner, P. G., Tsibris, J. C. M., Munck, E., p. 13. Engineering Experimental Stations, University of Illinois, Urbana 1969.
2. Malkin, R., Rabinowitz, J. C.: Ann. Rev. Biochem. **36**, 113 (1967).
3. Tagawa, K., Arnon, D. I.: Biochim. biophysica Acta **153**, 602 (1968).
4. Orme-Johnson, W. H., Hansen, R. E., Beinert, H.: Federat. Proc. **27**, 298 (1968).
5. — — — Ann. New York Acad. Sci. **158**, 336 (1969).
6. Mayhew, S. G., Petering, D., Palmer, G., Faust, G. P.: J. Biol. Chemistry **244**, 2830 (1969).

7. Tsibris, J.C.M., Tsai, R.L., Gunsalus, I.C., Orme-Johnson, W.H., Hansen, R.E., Beinert, H.: Proc. nat. Acad. Sci. USA **59**, 959 (1968).
8. — — — Biochim. biophys. Res. Comm. **30**, 323 (1968).
9. Sands, R.H.: In: Mössbauer spectroscopy in biological systems. Ed. by Debrunner, P.G., Tsibris, J.C.M., Munck, E., p. 16. Engineering Experimental Station, University of Illinois, Urbana 1969.
10. a) Moss, T.H., Petering, D., Palmer, G.: J. biol. Chemistry **244**, 2275 (1969).
b) Palmer, G.: Private Communication, Sept. 1, 1970.
11. Vartanian, D.V., Orme-Johnson, W.H., Hansen, R.E., Beinert, H., Tsai, R.L., Tsibris, J.C.M., Bartholomaus, R.C., Gunsalus, I.C.: Biochem. biophysic. Res. Commun. **26**, 569 (1967).
12. Hollocher, T.C., Solomon, F., Ragland, T.E.: J. biol. Chemistry **29**, 246 (1966).
13. Orme-Johnson, W.H., Hansen, R.E., Beinert, H., Tsibris, J.C.M., Bartholomaus, R.C., Gunsalus, I.C.: Proc. nat. Acad. Sci. USA **60**, 368 (1968).
14. Tsibris, J.C.M., Namtvedt, M.J., Gunsalus, I.C.: Biochem. biophysic. Res. Commun. **30**, 323 (1968).
15. Tsai, R.L., Tsibris, J.C.M., Gunsalus, I.C., Orme-Johnson, W.H., Hansen, R.E., Beinert, H.: In preparation (1970).
16. Benson, A.M., Yasunobu, K.T.: J. biol. Chemistry **244**, 955 (1969).
17. Keresztes-Nagy, S., Perini, F., Margoliash, E.: J. biol. Chemistry **244**, 981 (1969).
18. Matsubara, H., Sasaki, R.M., Chain, R.K.: J. biol. Chemistry **243**, 1725 (1968).
19. Sugeno, K., Matsubara, H.: Biochem. biophysic. Res. Commun. **32**, 951 (1968).
20. Lovenberg, W., Buchanan, B.B., Rabinowitz, J.C.: J. biol. Chemistry **238**, 3899 (1963).
21. Malkin, R., Rabinowitz, J.C.: Biochem. **5**, 1262 (1966).
22. Bayer, E., Eckstein, H., Hagenmaier, H., Josef, D., Koch, J., Krauss, P., Roder, A., Schretzmann, P.: Eur. J. Biochem. **8**, 33 (1969).
23. Tsibris, J.C.M., Tsai, R.L., Gunsalus, I.C.: Abstracts 154th Nat. Meeting Amer. chem. Soc., Chicago, C204.
24. Herriott, J.R., Sieker, L.C., Jensen, L.H., Lovenberg, W.: J. Molecular Biol. **50**, 391 (1970).
25. Jensen, L.H.: Private communication, Oct. 1970.
26. Beinert, H., Sands, R.H.: Biochem. biophysic. Res. Commun. **3**, 41 (1960).
27. Palmer, G., Brintzinger, H.P., Estabrook, R.W.: Biochem. **6**, 1658 (1967).
28. Gibson, J.F., Hall, D.O., Thornby, J.H.M., Whatley, F.R.: Proc. nat. Acad. Sci., USA **56**, 987 (1966).
29. Brintzinger, H., Palmer, G., Sands, R.: Biochem. **55**, 397 (1966).
30. Hall, D.O., Gibson, J., Whatley, F.: Biochem. biophysic. Res. Commun. **24**, 877 (1966).
31. Zerner, M., Gouterman, M., Kobayashi, H.: Theoret. chim. Acta (Berl.) **4**, 44 (1966).
32. Han, P.S., Das, T.P., Rettig, M.F.: Theoret. chim. Acta (Berl.) **16**, 1 (1970).
33. Wolfberg, M., Helmholz, H.: J. chem. Physics **20**, 837 (1952).
34. Pullman, A., Pullman, B.: Progress in Nucleic Acid Research and Molecular Biology **9**, 327 (1969).
35. Hoffman, R.: J. chem. Physics **40**, #9, 2480 (1964).
36. — Zeiss, G.D., Van Dine, G.W.J.: Amer. chem. Soc. **90**, 1485 (1968).
37. Zerner, M., Gouterman, M.: Theoret. chim. Acta (Berl.) **6**, 363 (1966).
38. Mulliken, R.S.: J. chem. Physics **23**, 1833, 2338, 2343 (1955).
39. Walsh, A.D.: J. chem. Soc. (London) 2260, 2288 (1953).
40. Loew, G.H.: Theoret. chim. Acta (Berl.) **20**, 203 (1971).
41. Pan, D.C., Allen, L.A.: J. chem. Physics **46**, #5, 1797 (1967).
42. Bearden, A.J., Dunham, W.R.: Structure and Bonding **8**, 1 (1970).
43. Ehrenberg, A.: Private Communication Aug. 1966.
44. Hoffmann, R.: J. chem. Physics **39**, 1397 (1963).
45. Kier, Lemont: MO consideration of amino acid conformation; MO studies in chemical pharmacology. New York: Springer Verlag 1970.
46. Hoyland, James: Semi-empirical MO Theories. A critique and review of progress; MO studies in chemical pharmacology. New York: Springer Verlag 1970.
47. Johnson, C.E., Bray, R.C., Commack, R., Hall, D.O.: Proc. nat. Acad. Sci. USA **63**, 1234 (1969).

Prof. Dr. G. Harris Loew
Department of Genetics
Stanford University Medical Center
Stanford, California 94305, USA